The Meteoritical Society

Meteoritics & Planetary Science 44, Nr 6, 805–821 (2009)
Abstract available online at http://meteoritics.org

^{40}Ar-^{39}Ar age determinations of lunar basalt meteorites Asuka 881757, Yamato 793169, Miller Range 05035, La Paz Icefield 02205, Northwest Africa 479, and basaltic breccia Elephant Moraine 96008

Vera A. FERNANDES[1, 2*], Ray BURGESS[2], and Adam MORRIS[2]

[1]Instituto Geofísico da Universidade de Coimbra, Av. Dias da Silva, 3000-134 Coimbra, Portugal
[2]School of Earth, Atmospheric and Environmental Sciences, University of Manchester, Oxford Road, Manchester M13 9PL, UK
[*]Present address: Berkeley Geochronology Center and Department of Earth and Planetary Sciences, University of California at Berkeley, Berkeley, California, USA
[*]Corresponding author. E-mail: veraafernandes@yahoo.com

(Received 27 October 2008; revision accepted 15 March 2009)
Supplemental material is available online at http://meteoritics.org/Online%20Supplements.htm

Abstract–^{40}Ar-^{39}Ar data are presented for the unbrecciated lunar basaltic meteorites Asuka (A-) 881757, Yamato (Y-) 793169, Miller Range (MIL) 05035, LaPaz Icefield (LAP) 02205, Northwest Africa (NWA) 479 (paired with NWA 032), and basaltic fragmental breccia Elephant Moraine (EET) 96008. Stepped heating ^{40}Ar-^{39}Ar analyses of several bulk fragments of related meteorites A-881757, Y-793169 and MIL 05035 give crystallization ages of 3.763 ± 0.046 Ga, 3.811 ± 0.098 Ga and 3.845 ± 0.014 Ga, which are comparable with previous age determinations by Sm-Nd, U-Pb Th-Pb, Pb-Pb, and Rb-Sr methods. These three meteorites differ in the degree of secondary ^{40}Ar loss with Y-793169 showing relatively high Ar loss probably during an impact event ~200 Ma ago, lower Ar loss in MIL 05035 and no loss in A-881757. Bulk and impact melt glass-bearing samples of LAP 02205 gave similar ages (2.985 ± 0.016 Ga and 2.874 ± 0.056 Ga) and are consistent with ages previously determined using other isotope pairs. The basaltic portion of EET 96008 gives an age of 2.650 ± 0.086 Ga which is considered to be the crystallization age of the basalt in this meteorite. The Ar release for fragmental basaltic breccia EET 96008 shows evidence of an impact event at 631 ± 20 Ma. The crystallization age of 2.721 ± 0.040 Ga determined for NWA 479 is indistinguishable from the weighted mean age obtained from three samples of NWA 032 supporting the proposal that these meteorites are paired. The similarity of ^{40}Ar-^{39}Ar ages with ages determined by other isotopic systems for multiple meteorites suggests that the K-Ar isotopic system is robust for meteorites that have experienced a significant shock event and not a prolonged heating regime.

INTRODUCTION

Since 1999, the lunar sample collection has been supplemented with about 140 stones from the Moon. Many of these stones are paired, and the total number of different lunar meteorites is currently 64 (http://meteorites. wustl.edu/lunar/moon_meteorites_list_alumina.htm). Of these 16% (10) are mare basalts, which corresponds well with the ~17% of the lunar surface covered by maria. When major- and trace-element compositions of the lunar basaltic meteorites are compared with mare basalts collected by the Apollo and Luna missions (Fig. 1), it is apparent that most of the basaltic meteorites are from regions of maria that were not sampled during missions. The majority of Apollo and Luna basalts are mainly low or high Ti basalts with ages in the range of 3.1–3.8 Ga with modes at 3.2–3.3 Ga and 3.6–3.7 Ga. In contrast, lunar basaltic meteorites are low or very low Ti (VLT) basalts with ages between 2.8–4.3 Ga (Fernandes et al. 2003; Borg et al. 2004; Terada et al. 2007a; Shih et al. 2008; and Sokol et al. 2008). Hagerty et al. (2006) have shown that low Ti basalts are from lunar mantle sources with relatively high radioactive heat production, thus enabling them to sustain melting over longer timescales and able to generate basalts of comparatively young age.

In this study, the ^{40}Ar-^{39}Ar dating method was applied to five lunar basalt meteorites: Asuka (A-) 881757, Yamato (Y-) 793169, Miller Range (MIL) 05035, LaPaz Icefield (LAP) 02205, Northwest Africa (NWA) 479, and one basaltic/gabbroic breccia, Elephant Moraine (EET) 96008,45. The aim is to determine the crystallisation age of the basalts, and

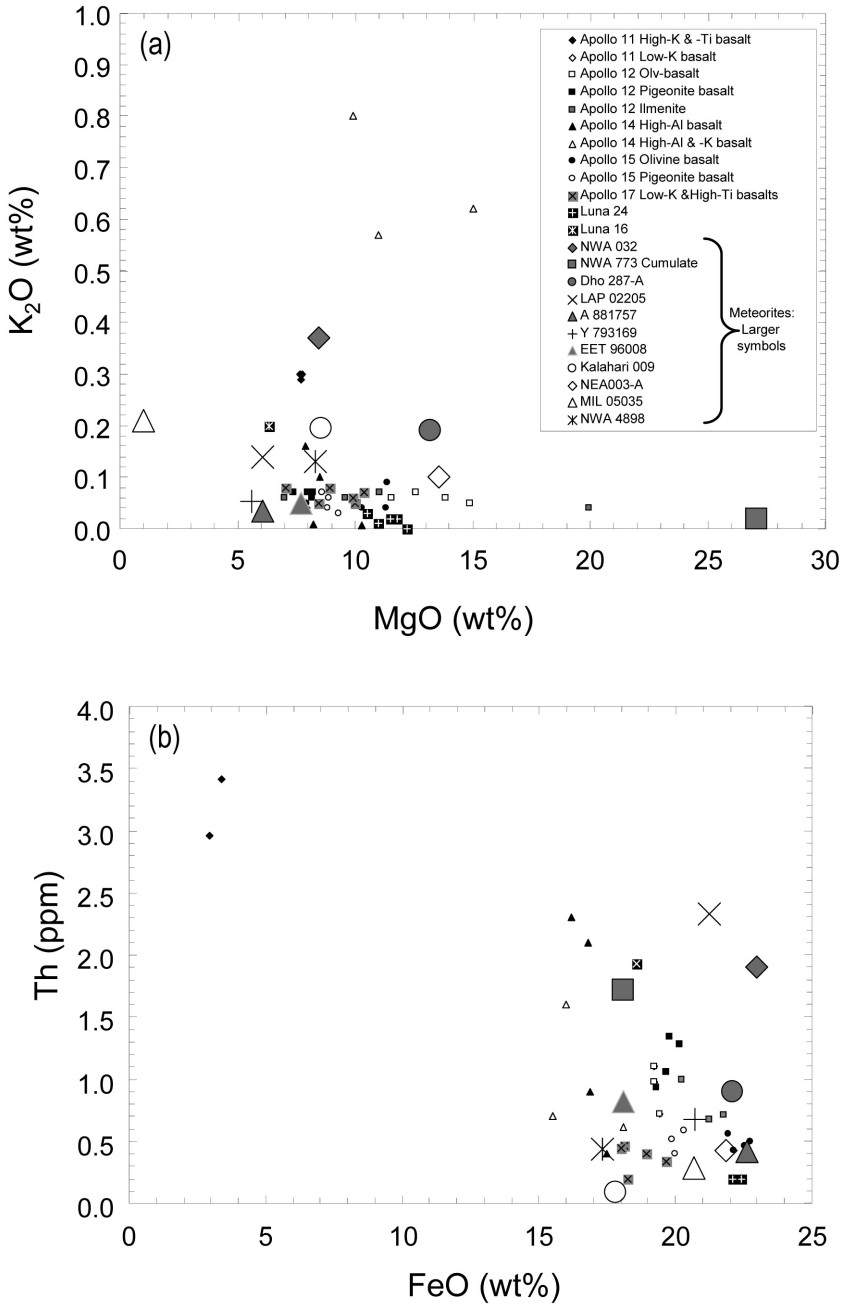

Fig. 1. Bulk composition of basaltic lunar mare meteorites (NWA 032, NWA 773 cumulate, Dhofar 287-A, LAP 02205, A-881757, Y-793169, EET 96008, Kalahari 009, MIL 05035, and NWA 4898) compared to Apollo and Luna basalts. Same symbols for both plots: a) MgO (wt%) versus K_2O (wt%), b) FeO (wt%) versus Th (ppm). Data from: Fagan et al. (2002), Jolliff et al. (2003), Anand et al. (2003), Joy et al. (2008), Yanai et al. (1993), Koeberl et al. (1993), Yanai and Kojima (1991), Mikouchi (1999), and Warren and Kallemeyn (1993), Sokol et al. (2008), Haloda et al. (2009), Joy et al. (2007), Greshake et al. (2008), and J. A. Barrat (personal communication).

the timing of any major impact event(s) that may have disturbed their K-Ar systems. The age information obtained can be used to help assess relationships between groups of meteorites related on other chemical and petrologic criteria, especially those which are launch paired, and to help constrain source areas on the Moon from which the meteorites derived.

SAMPLE DESCRIPTIONS

In this section we give a brief description of each meteorite based mainly upon literature. Previously determined ages are given in Table 1 and are discussed in relation to the Ar-Ar ages determinations in section Summary of Ages and Comparison with Literature Data. For LAP

Table 1. Summary of published ages (in Ga).

	Y-793169	A-881757	MIL 05035	LAP 02205	EET 96008	NWA 032
Ar-Ar	3.987 ± 0.015[a,e]	3.79 ± 0.02[f,g]		2.95 ± 0.04 l		2.78 ± 0.06[p]
	3.257 ± 0.008[b,e]	3.81 ± 0.02[f,h]				
	0.751 ± 0.004[c,e]					
	3.9–4.3[d,e]					
K-Ar		3.10 ± 0.6[g]				
Pb-Pb	3.919 ± 0.0.09[4e]	3.940 ± 0.028[f]				
Sm-Nd	3.43 ± 0.19 [e]	3.87 ± 0.06[f]	3.80 ± 0.05[j]	3.15 ± 0.04[l]		2.69 ± 0.16[q]
Rb-Sr		3.84 ± 0.03[f]	3.90 ± 0.04[k]	3.02 ± 0.03[l]		2.852 ± 0.065[q]
				2.99 ± 0.02[m]		
Th-Pb	3.15 ± 0.51[e]	3.82 ± 0.29[f]				
U-Pb	3.81 ± 0.22[e]	3.940 ± 0.009[f,i]		2.93 ± 0.15[n]	3.53 ± 0.27[o]	
		3.850 ± 0.150f			3.52 ± 0.10[o]	
Pu-Xe		4.24 ± 0.17[i]				

[a]Plagioclase fusion. [b]Plagioclase total gas age. [c]Impact event. [d]High-temperature apparent ages. [e]Torigoye-Kita el al. (1995). [f]Misawa et al. (1993). [g]Glass step-heating. [h]plagioclase step-heating..[i]U-Pb concordia. [j]Thalmann et al. (1996). [k]Nyquist et al. (2007). [l]Nyquist et al (2005). [m]Rankenburg et al. (2007). [n]Anand et al. (2006). [o]Terada et al. (2005). [p]Fernandes et al. (2003). [q]Borg et al. (2007).

02205 and EET 96008 there was sufficient sample that we were able to prepare polished sections for petrographic and chemical characterization using scanning electron microscopy (SEM) and electron microprobe analysis (EMPA) prior to Ar-Ar age determination. The results of sample characterization are discussed in the relevant sections that follow.

The mare basalt meteorites Y-793169, A-881757, and MIL 05035 (together with basaltic regolith breccia-bearing ferroan anorthosite MET 01210) share many petrologic, chemical, isotopic and age similarities and are collectively referred to as the YAMM group (Arai et al. 2007; Zeigler et al. 2007; Joy et al. 2008). Arai et al. (2007) suggest that the YAMM group of meteorites may represent a volcano-stratigraphic sequence consisting of an upper regolith environment underlain by a coarsening of the basalt flows from top to bottom.

A-881757 was found in the NE of the Nansen ice field, ~130 km south of the Japanese Asuka station in Antarctica (Yanai 1991). This meteorite is classified as a gabbroic mare basalt (Yanai 1991; Yanai et al. 1993; Koeberl et al. 1993) and is more coarse-grained than Y-793169. Pyroxene grains in A-881757 are up to 4 mm across and maskelynite and ilmenite are up to 3 mm across. Maskelynite is typically 1.0 × 0.2 mm and the meteorite has a subophitic texture (Yanai and Kojima 1991; Arai et al. 1996). Pyroxene is the most abundant mineral with compositions ranging from $En_{7.8–43.6}$, $Fs_{30.7–68.2}$, to $Wo_{11.6–40.9}$ (Table 2). Also present are ilmenite, troilite, and traces of olivine (in symplectites, and iron-rich ranging from $Fa_{86.6}$ to $Fa_{94.6}$), apatite, silica phase (quartz), and nickel-iron (Yanai et al. 1993; Koeberl et al. 1993). The range of plagioclase composition of $An_{74–90}$ is similar to that found in Y-793169, however most analyses show a more restricted range of $An_{90–95}$ (Table 2). Koeberl et al. (1993) described the existence of brownish and greenish glassy melts having similarities to Apollo 17 and Luna VLT basalts, which was also supported by their trace element data. Previous age determinations of A-881757 using different isotope chronometers show a general concordance at between 3.8–3.9 (Table 1; Misawa et al. 1993).

Y-793169 was found in the Minami-Yamato Nunataks Mountains, Antarctica, and is an unbrecciated, crystalline, subophitic low titanium basalt, with Fe-rich pyroxene, plagioclase, and dark mesostasis (Yanai and Kojima 1991; Takeda et al. 1993). Detailed mineralogical and compositional studies have been reported by Takeda et al. (1993), Yanai and Kojima (1991), Mikouchi (1999a) and Warren and Kallemeyn (1993). Pyroxene crystals are fractured and, together with the partly maskelynitized plagioclase, indicate that some degree of shock has been experienced by the meteorite, but the overall texture is reported as not being disturbed (Takeda et al. 1993). The feldspars are Ca-rich, ranging from $An_{88–97.5}$ (Table 3 and Yanai and Kojima 1991) but mostly between An_{92-94}; pyroxene compositions are variable, $En_{1.9–53.5}$, $Fs_{22.2–84.3}$, and $Wo_{9.7–40.7}$ (Table 2). Olivine is iron-rich at $Fa_{98.5}$, although the composition of only a single grain has been reported (Yanai and Kojima 1991). In addition to the diaplectic glass identified by Torigoye-Kita et al. (1995), the presence of melt glass has also been reported in Y-793169 (Mikouchi 1999a). Previous age determinations of Y-793169 are discordant ranging between 3.4–4.1 Ga (Table 1; Torigoye-Kita el al., 1995). Y-793169 and A-881757 have been paired on the basis of cosmic ray exposure history (Nishiizumi et al. 1992), bulk chemistry (having higher Ti content than VLT basalts) and in particular the enrichment in heavy REE (Koeberl et al. 1993; Warren and Kallemeyn 1993). Both have experienced similar levels of shock converting plagioclase to maskelynite, however subsequent thermal annealing appears to have caused re-crystallization of plagioclase in Y-793169 (Mikouchi 1999). Based on mineralogical data, Takeda et al. (1993) have suggested that crystallization trends imply that Y-

Table 2. Summary of plagioclase and pyroxene chemical composition (wt%) determined by electron microprobe analyses for lunar meteorites A-881757, Y-793169, LAP 02205, EET 96008, and MIL 05035.

	A-881757[a]			Y-793169[a]				LAP 02205			EET 96008		MIL 05035	
	Plag.	Pyrox.		Plag.		Pyrox.		Plag.	Pyrox.		Plag.	Pyrox.	Plag.	Pyrox.
		Core	Rim	Core	Rim	Core	Rim		Core	Rim				
SiO_2	44.50	50.84	48.88	45.57	48.11	51.58	49.03	48.76	49.64	46.01	44.32	50.91	46.09	49.84
TiO_2	0.01	0.95	0.96	–	–	0.814	1.10	0.06	1.22	0.98	0.02	0.46	0.03	0.87
Al_2O_3	35.31	1.94	0.90	33.80	31.87	2.54	1.17	30.75	2.01	0.82	34.75	1.26	34.45	1.36
Cr_2O_3	0.01	0.72	0.12	0.01	0.01	0.837	0.03	–	0.58	0.08	<0.02	0.52	<0.02	0.38
MgO	0.09	12.86	2.39	0.14	0.02	15.57	6.08	0.04	14.47	1.62	0.09	15.81	0.09	9.93
CaO	18.84	11.51	18.29	18.95	17.31	11.48	10.79	17.08	9.40	9.39	19.43	8.65	18.35	11.08
MnO	0.04	0.38	0.26	0.01	0.05	0.461	0.42	0.02	0.38	0.53	<0.02	0.35	<0.02	0.53
FeO	0.29	21.62	29.36	0.60	0.97	17.75	32.07	1.75	22.97	40.80	0.40	22.28	0.67	24.67
Na_2O	0.54	<0.02	0.05	0.68	1.21	<0.02	0.02	1.32	<0.02	<0.02	0.62	0.04	1.01	0.05
K_2O	0.01	<0.02	<0.02	0.02	0.16	<0.02	0.02	0.30	<0.02	<0.02	0.04	<0.02	0.03	<0.02

[a]Arai, T. (unpublished data).

Table 3. Summary of typical blank levels and their variability (2σ) over the course of these experiments for each meteorite, in units of 10^{-14} cm^3 STP (furnace blanks are in 10^{-13} cm^3 STP), are equivalent to.

	^{40}Ar	^{39}Ar	^{38}Ar	^{37}Ar	^{36}Ar
IR					
A-881757	2668.4 ± 5.7	10.4 ± 0.1	17.6 ± 0.1	43.3 ± 0.8	52.9 ± 0.7
Y-793169	2533.3 ± 84.4	9.4 ± 2.3	16.4 ± 2.8	40.0 ± 2.1	48.6 ± 3.3
LAP 02205	782.0 ± 12.0	58.7 ± 0.9	19.3 ± 0.3	74.6 ± 1.1	26.2 ± 0.4
EET 96008	1167.2 ± 87.7	86.6 ± 10.1	25.1 ± 11.7	99.2 ± 11.7	38.8 ± 6.3
Furnace					
Y-793169	[a]11932.0 ± 24.8	11.4 ± 13.5	11.3 ± 6.4	2.4 ± 1.8	42.4 ± 15.8
	[b]39804.5 ± 103.9	13.5 ± 3.8	28.1 ± 3.1	4.7 ± 11.7	142.5 ± 4.3
NWA 479	[a]9922.4 ± 53.1	10.4 ± 30.1	10.0 ± 9.6	28.6 ± 170.9	34.5 ± 10.2
	[b]127466.6 ± 15.5	7.1 ± 5.2	19.9 ± 8.5	2.9 ± 10.0	90.0 ± 4.0

[a]Blank at low temperature (300–1000 °C).
[b]Blank at high temperature (≥1100 °C).

793169 formed near the surface under disequilibrium growth conditions, and that A-881757 crystallized at depth under conditions closer to equilibrium conditions, in a similar lava unit and developed a coarser texture.

MIL 05035 was found in the Miller Range in eastern Transantarctic Mountains. MIL 05035 is a coarse-grained VLT mare gabbro comprising pyroxene, plagioclase and mesostasis (Arai et al. 2007; Ziegler et al. 2007; Joy et al. 2008). The anorthite content shows a narrow range between An_{89} and An_{92} (Table 2) and the pyroxene composition is $En_{19–37}$, $Fs_{28–56}$, and $Wo_{16–37}$ (Table 2). Based on the petrographic description of Joy et al. (2008), MIL 05035 pyroxene grains usually display undulatory extinction and show weak mosaicism or localized shock-induced twinning, and fine (sub-micron) planar deformation features. Plagioclase is completely converted to maskelynite (Arai et al. 2007; Joy et al. 2008). These shock-induced features suggest that the sample underwent shock pressures of 28–34 GPa (shock stage 2b of Stöffler and Grieve 2007). The bulk TiO_2 content of MIL 05035 (0.9 wt%, Joy et al. 2008) places this basalt between the low-Ti and VLT groups and it also has low incompatible trace element concentrations. Petrogenetic modeling of MIL 05035 suggests that this basalt cooled in a shallow environment (Joy et al. 2008), and this is supported by the presence of unequilibrated pyroxenes and symplectite assemblages similar to those found in A-881757 (Arai et al. 1996). Nyquist et al. (2007) have determined the Sm-Nd and Rb-Sr ages of MIL 05035 at between 3.80–3.90 Ga (Table 1).

LAP 02205 was found during the ANSMET (Antarctic Search for Meteorites) season of 2002–03 in the La Paz ice fields, ~400 km from the South Pole, in the middle of the Antarctic plateau. This meteorite has been classified as a coarse-grained unbrecciated lunar mare basalt dominated by large crystals of plagioclase (100–600 μm) and pyroxene (100–500 μm), with minor amounts of olivine grains and mesostasis areas consisting of (primarily) ilmenite, fayalite, cristobalite and glass (McBride et al. 2003; Mikouchi et al. 2004; Righter et al. 2005; Anand et al. 2006; Joy et al. 2006). Glass veins, presumably related to shock also permeate this meteorite.

The sample of LAP 02205 used in this study (Fig. 2a) contains a region of mesostasis which includes a SiO_2-rich glass (98–99 wt% SiO_2) vein (labelled 'V' in Fig. 2a), FeSi, and ilmenite (<5 μm). Spinels (Cr-spinel and ulvöspinel) and fayalite olivine are also found in small amounts. The bulk composition of LAP 02205 places it in the category of low Ti (TiO_2 = 3.86 wt%) and slightly aluminous basalt (Zeigler

et al. 2005; Anand et al. 2006; Joy et al. 2006). The plagioclase laths are partially to totally converted to maskelynite (Righter et al. 2005; Zeigler et al. 2005) often containing fractured areas (plagioclase) and smooth areas (maskelynite), often within the same grain. No compositional difference between the plagioclase and maskelynite was noted (Zeigler et al. 2005). The plagioclase composition is $An_{89–93}$ which is within the range found previously (Zeigler et al. 2005; Joy et al. 2006). The pyroxenes also show shock features (fractures), but they are not as obvious as those of plagioclase crystals. The chemical composition of the pyroxenes in the sample analysed (Fig. 2b; Table 3) is identical to that studied previously (Zeigler et al. 2005; Anand et al. 2006; Joy et al. 2006), showing magmatic zoning with cores richer in Mg than the rims (typical core $En_{35.3}$ and rim $En_{0.9}$) and the composition is variable with a range of $En_{4–28}$ $Fs_{59–79}$ $Wo_{9–35}$ suggesting a pigeonite to subcalcic augite composition (Zeigler et al. 2005). Opaque phases include trace amounts of ilmenite, chromite, and ulvöspinel.

NWA 479 is paired with lunar mare basalt meteorite NWA 032 (Barrat et al. 2005). It is an unbrecciated basalt with a porphyritic texture in a matrix of radiating pyroxene and feldspar crystals. The plagioclase has a composition $An_{80–90}$ (Barrat et al. 2005). Olivines occur as phenocrysts that make up ~12 vol% of the meteorite and are up to 300 μm in size (Fagan et al. 2002; Barrat et al. 2005). Olivine has Mg-rich cores ($Fo_{55–67}$) with sometimes discontinuous Fe-rich rims ($Fo_{15–55}$; Barrat et al. 2005). Pyroxenes occur as phenocrysts comprising ~5 vol% (Fagan et al. 2002; Barrat et al. 2005) and are mostly ferroan augites to pigeonites of composition $En_{15–34}Fs_{45–66}Wo_{19–31}$. Those in the matrix show extensive zoning and are rimmed by pigeonite, close to Mg-free and pyroxferroite. The bulk composition of NWA 032/479 does not overlap that of any known mare basalts (Fig. 1), but is similar to Apollo 15 olivine basalt, and the olivine phenocrysts abundance is similar to that in Apollo 12 olivine basalts (Fagan et al. 2002). It shows low-Ti and lower MgO composition, and higher olivine phenocryst abundance than other mare basalt samples.

EET 96008 is a breccia dominated by basaltic mineral phases, with minor highland material and lithic clasts (Fig. 3; Anand et al. 2003). Mikouchi (1999b) describes this meteorite as a fragmental breccia mainly composed of pyroxene, plagioclase and olivine (≤1.5 mm) clasts set in a fine-grained dark matrix with a few different compositional types of glass, cementing the matrix and occurring as veins. Anand et al. (2003) suggest that the bulk rock major, trace and REE element contents of EET 96008 are similar to those observed for VLT basalts that have experienced extreme fractional crystallisation near the silicate-liquid immiscibility boundary. Warren and Ulff-Møller (1999) suggested that the mare component of this meteorite originated either as a shallow intrusion, or as an unusually deep-ponded flow. The section used in this study shows two different textures (Fig. 3), a brecciated region, and an area with a preserved gabbroic

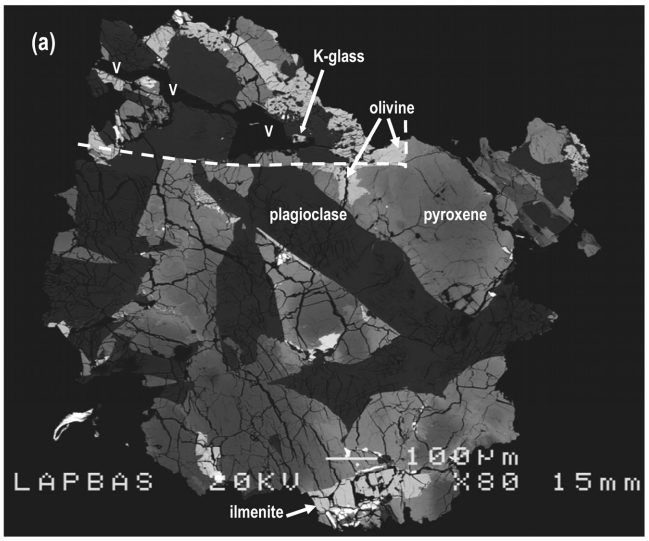

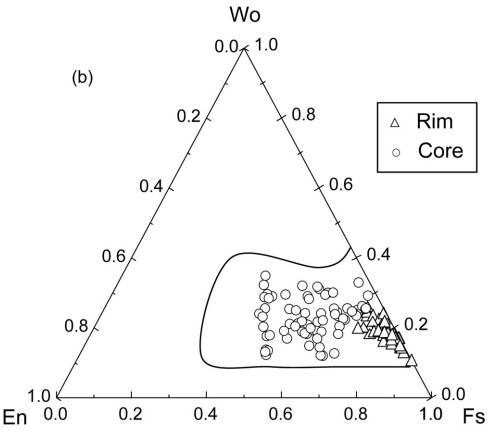

Fig. 2. a) Backscattered electron image of LAP 02205. The dashed line shows the area containing mesostasis and a SiO_2-glass vein (V), FeSi, FeS, together with ilmenite (<5 μm) and K-glass, and glass with composition showing mixing between plagioclase and pyroxene. b) Pyroxene compositions determined for LAP 02205. Enclosed area corresponds to pyroxene data obtained by Jolliff et al. (2004), Zeigler et al. (2005), Anand et al. (2005), and Joy et al. (2006).

texture composed mainly of plagioclase (~400 μm) and pyroxene (~400 μm), but also with minor olivine. The chemical composition of the pyroxene in the breccia and basalt portions of EET 96008 is the same $En_{20–39}Fs_{31–68}Wo_{6–41,}$ corresponding to pigeonite and ferroaugites similar to those reported by Anand et al. (2003). The large pyroxene crystals in the basalt show exsolution lamellae superposed by shock related cracks. These lamellae are atypical for mare basalts (Warren and Ulff-Møller 1999) and indicate slow cooling. The plagioclase shows a narrow compositional range of $An_{94–98}$ similar to that reported by Anand et al. (2003) which these authors attributed to a highland component. The mare component of EET 96008 has textural, mineral and geochemical similarities to low Ti and VLT basalts (Warren and Ulff-Møller 1999; Anand et al. 2003).

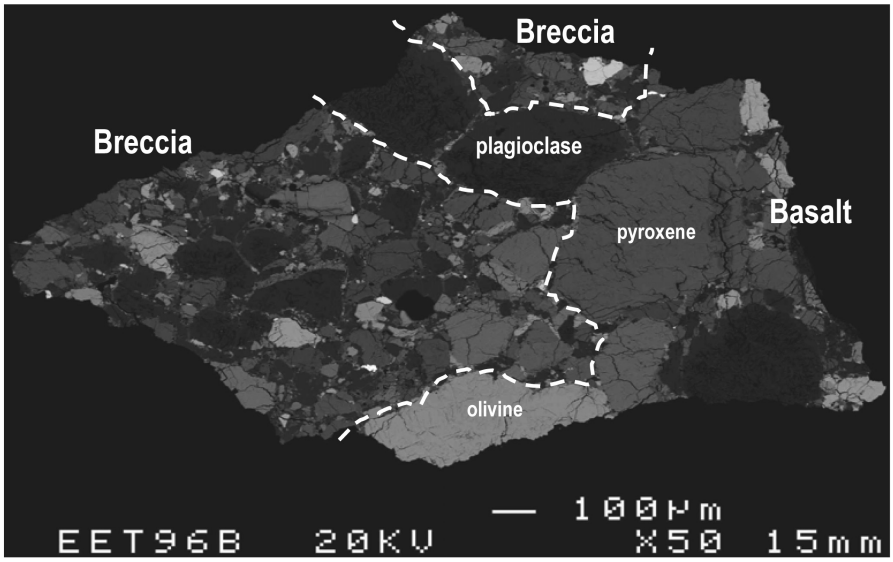

Fig. 3. Backscattered electron image of EET 96008. The dashed line illustrates the boundary between breccia and basalt components.

EXPERIMENTAL METHODS

Bulk, plagioclase and pyroxene separates of A-881757 and Y-793169 were obtained by hand-picking under a binocular microscope. Some glass was also believed to be present in the pyroxene fraction of A-881757. Only bulk samples were analyzed of MIL 03035 and NWA 479.

Fragments of LAP 02205 and EET 96008 were cut and polished for sample characterization using scanning electron microscopy (SEM) and electron microprobe analysis (EMPA). Mineral chemical analyses (pyroxene, olivine, plagioclase, maskelynite, ilmenite, glassy vein and associated phases) of LAP 02205 and EET 96008, and compositional profiles of pyroxenes in LAP 02205 were obtained using a five-spectrometer CAMECA SX100 electron microprobe with on-line data reduction. A cup current of 10–20 nA with an acceleration potential of 15 KeV and an electron beam diameter of <5 μm was used for individual mineral analyses. Backscattered electron images of LAP 02205 and EET 96008 were acquired for preliminary characterization of these meteorites using a JEOL 6400 scanning electron microscope (SEM). Following SEM and EMPA study, both sections were cleaned of adhesive by immersion in acetone for ≧48 h, and inspected under the binocular microscope to remove any remaining adhesive material. The LAP 02205 section was then subdivided into basalt and vein-rich fragments (Fig. 2), and EET 96008 was subdivided into breccia and basalt lithologies (Fig. 3) in preparation for Ar-Ar analysis.

All six meteorites were irradiated with a fast neutron flux of between 2–3 × 10^{18} neutrons cm^{-2} in position B2W at the SAFARI-1 reactor at Pelindaba, South Africa. Samples were positioned between Hb3gr monitors in silica glass vials. Errors on Ar-Ar ages includes the 1% difference in J value obtained for the monitors and the uncertainty on the age determination of the Hb3gr monitor (1073.6 ± 4.6 Ma, Jourdan et al. 2006; Schwarz and Trieloff 2007) ^{40}Ar-^{39}Ar analysis of Y-793169 and A-881757 were carried out 11 months after irradiation during which time the Ca-derived ^{37}Ar had almost completely decayed. Calcium contents derived from levels of ^{37}Ar in these meteorites are therefore considered to be semi-quantitative.

Argon gas was extracted from the samples by stepped heating using either a resistance furnace (MIL 05035 and NW A479) or infra-red (IR) laser (A-881757, Y-793169, LAP 02205, and EET 96008). The IR laser consists of a Nd-YAG continuous wave laser (λ = 1064 nm) with a defocused beam of 3 mm diameter used to heat samples from 0.5 to 15W laser output power in 16–34 heating steps each for 1 minute.

During furnace stepped heating Ar was released over the temperature interval 400–1600 °C using steps of 100 °C or 50 °C and 30 min. duration. Typical blank levels and their variability (2σ) over the course of these experiments are given in Table 3. All furnace blanks have an approximately atmospheric argon isotopic composition. Data have been corrected for blanks, mass discrimination and neutron interference isotopes. Ar-Ar ages are reported at the two standard deviation (2σ) level of uncertainty. Further details of the experimental methods and data reduction procedures are given in Burgess and Turner (1998), Fernandes et al. (2000) and Fernandes and Burgess (2005).

RESULTS AND DISCUSSION

Ar-Ar Age Determination

Ar-Ar data for A-881757, Y-793169, MIL 05035, LAP 02205, EET 96008, and NWA 479 are shown as apparent age and Ca/K (derived from $^{37}Ar_{Ca}/^{39}Ar_{K}$) spectra, and, where

Table 4. Summary of ^{40}Ar-^{39}Ar age results for lunar basalt meteorites analyzed in this study. Errors are 2σ level of uncertainty.

Sample	Weight (mg)	K (ppm)[a]	Ca (%)[a]	Age (Ga)	CRE (Ma)
A-881757					
Plagioclase	5.24	19 ± 2	nd	3.650 ± 0.048	–
Pyroxene	3.11	95 ± 4	nd	3.699 ± 0.056	–
Bulk	3.10	377 ± 11	nd	3.763 ± 0.046	–
Y-793169					
Plagioclase	1.70	210 ± 6	nd	3.811 ± 0.098[b] 0.410 ± 0.022[c]	–
Pyroxene+glass	3.39	272 ± 9	nd	0.203 ± 0.042[c]	–
Bulk	5.05	1030 ± 30	nd	3.811 ± 0.098[b] 0.363 ± 0.016[c]	–
MIL 05035					
Bulk-1	9.23	244 ± 2	15.3 ± 0.1	3.910 ± 0.012 1.638 ± 0.098[c]	1–3
Bulk-2 (BGC)[d]	3.85	162 ± 1	0.16 ± 0.01	3.845 ± 0.014	–
LAP 02205					
Bulk	2.36	53 ± 1	0.80 ± 0.02	2.985 ± 0.016	43 ± 7
Basalt	0.26	485 ± 1	1.82 ± 0.03	2.889 ± 0.044	–
Mesostasis/vein	0.32	434 ± 1	3.29 ± 0.04	2.874 ± 0.056	–
NWA 479					
Bulk	5.90	949 ± 27	6.78 ± 0.19	2.721 ± 0.040	275 ± 8
EET 96008					
Bulk	4.42	23 ± 1	0.66 ± 0.01	3.23 ± 0.118 0.631 ± 0.020[c]	10 ± 1
Breccia	0.34	54 ± 5	2.40 ± 0.59	3.755 ± 0.171	–
Basalt	0.75	6 ± 1	2.01 ± 021	2.650 ± 0.086	–

[a]K and Ca content reported were calculated based on the total ^{39}Ar and ^{37}Ar released during laser heating.
[b]Max. apparent age, minimum crystallization age.
[c]Min. apparent age due to impact event.
[d]BGC = Berkeley Geochronology Center.
nd = not determined.

linear correlations occur, as $^{40}Ar/^{36}Ar$ versus $^{39}Ar/^{36}Ar$ plots (Figs. 4–9). Age data are summarized in Table 4. All uncertainties shown in the figures and for quoted ages are at the 2σ level.

A-881757

The Ar-Ar age and Ca/K spectrum diagrams for plagioclase, pyroxene and bulk samples of A-881757 are shown in Fig. 4a. A881757 contains negligible trapped argon components ($^{40}Ar/^{36}Ar$ ~0) as indicated by the linear correlation on a $^{40}Ar/^{36}Ar$ versus $^{39}Ar/^{36}Ar$ plot (Fig. 4b). The age spectra show relatively flat patterns for the bulk and plagioclase samples with integrated ages of 3.763 ± 0.046 Ga (90% $^{39}Ar_K$ release) and 3.650 ± 0.048 Ga (98% $^{39}Ar_K$ release), respectively (Table 4). The pyroxene-separates show a decrease in apparent age at high temperature, a feature previously observed by Misawa et al. (1993), and likely related to ^{39}Ar recoil during irradiation. An age of 3.699 ± 0.056 Ga from 80% of the $^{39}Ar_K$ release is calculated for the pyroxene. Because samples were analyzed 11 months after irradiation, ^{37}Ar had decayed to low levels making Ca/K ratios only approximate. The plagioclase separate has a relatively constant Ca/K ratio of 430–600 which is within range the values obtained for plagioclase/maskelynite (T. Arai, personal communication; Table 2). Pyroxene and bulk A-881757 show a wider range of Ca/K ratio of 120–4130, and 50–250 respectively, both show an increase from low to high temperature steps, suggesting release from a mixture of mineral phases, or from chemically zoned pyroxene grains.

Y-793169

The Ar-Ar age and Ca/K spectrum diagrams for bulk and mineral separates of Y-793169 samples are shown in Fig. 5. Samples contain negligible amounts of trapped solar or lunar Ar as indicated by the low level of ^{36}Ar released during step heating. Even if it is assumed that all the measured ^{36}Ar released during each temperature step has a trapped $^{40}Ar/^{36}Ar$ of between 1 and 3, then apparent ages are only reduced by <1%, well within the 2σ errors of individual step ages. Due to the presence of negligible trapped Ar and uncertainties

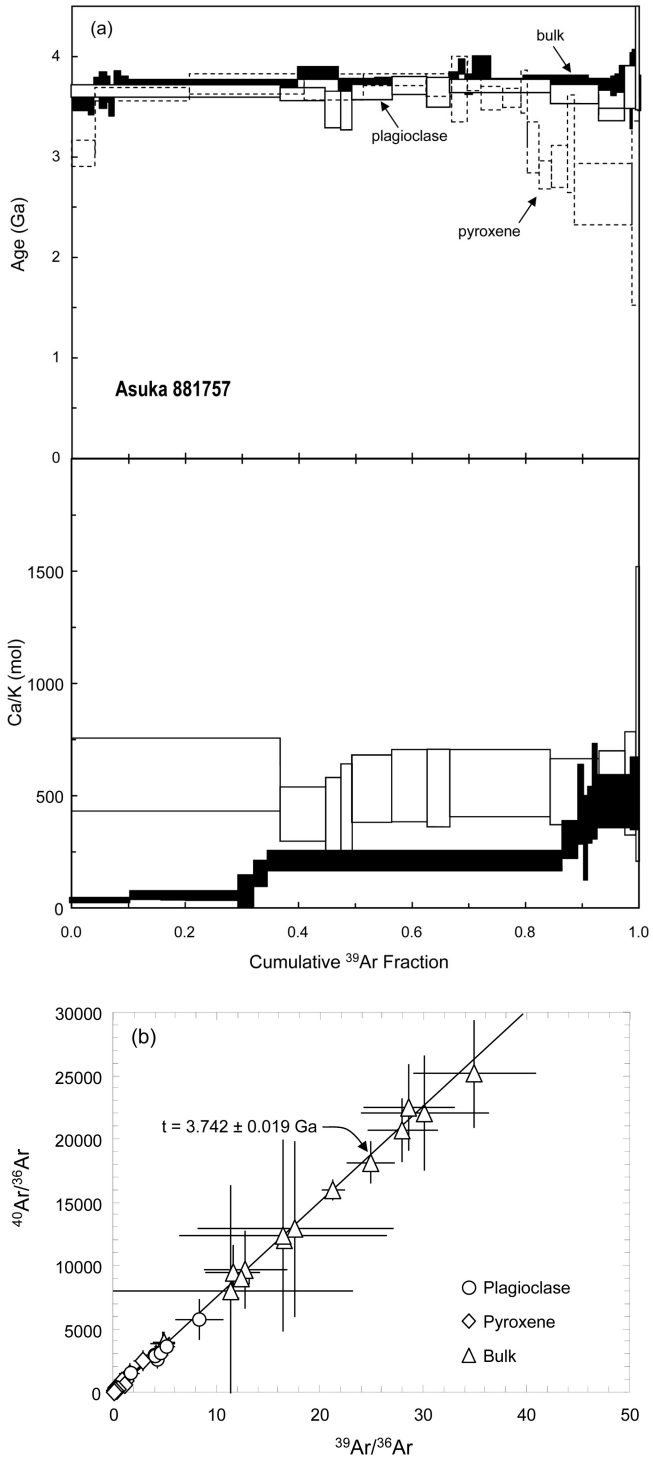

Fig. 4. Ar-Ar results for A-881757 bulk, pyroxene and plagioclase samples. (a) apparent age and Ca/K spectra, and (b) ^{40}Ar/^{36}Ar versus ^{39}Ar/^{36}Ar diagram.

regarding its isotopic composition, no attempt has been made to correct for this component in calculating the apparent ages shown in Fig. 5 and summarized in Table 4.

The age spectra for bulk and plagioclase samples show

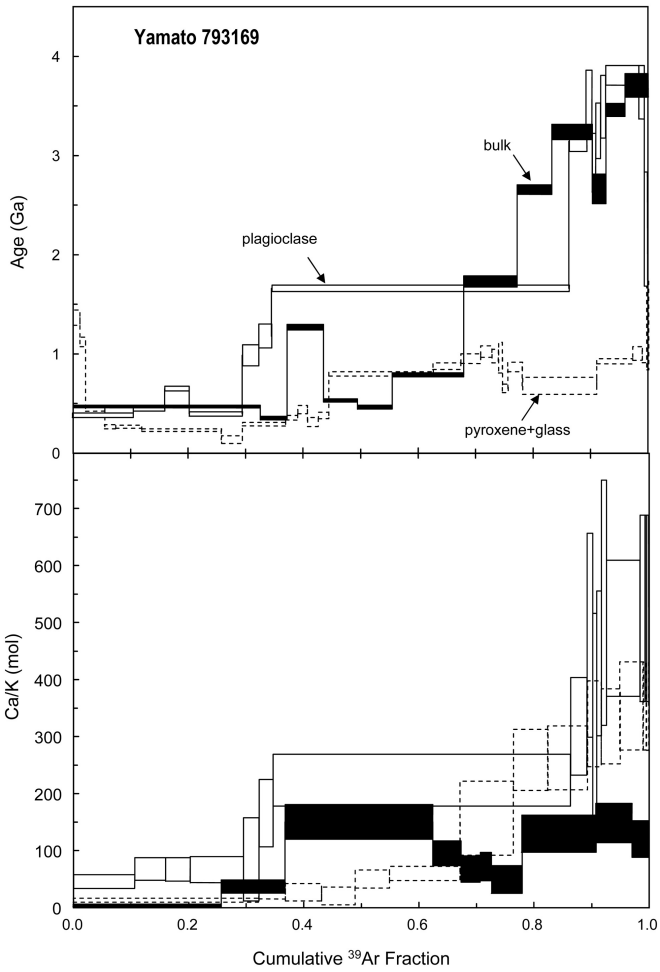

Fig. 5. Apparent age and Ca/K spectrum diagrams for Y-793169 bulk, pyroxene, and plagioclase samples.

similar complex patterns (Fig. 5), the initial ~55% $^{39}Ar_K$ release for bulk and ~30% for plagioclase, show low apparent ages indicative of Ar loss during a disturbance between 203–410 Ma. At intermediate to high temperatures the apparent ages for both bulk and plagioclase progressively increase to maximum ages of 3.691 ± 0.060 Ga and 3.811 ± 0.044 Ga, respectively. Due to the disturbed age spectra, the maximum apparent age of 3.811 ± 0.044 Ga obtained from the plagioclase separate is interpreted to be the minimum crystallization age for this meteorite.

The age spectrum for pyroxene does not show such a steep increase in apparent age with temperature as observed for the bulk and plagioclase samples. A low apparent age of 203 ± 42 Ma was obtained at ~29% ^{39}Ar release at low temperature from pyroxene. There is an increase in apparent ages after ~44% $^{39}Ar_K$ release to a maximum of between 800–900 Ma (Fig. 5). The low apparent ages of pyroxene is difficult to explain, however we suspect that our sample was contaminated with fragments of shock glass, which is visually similar to pyroxene and would contain a higher level of K,

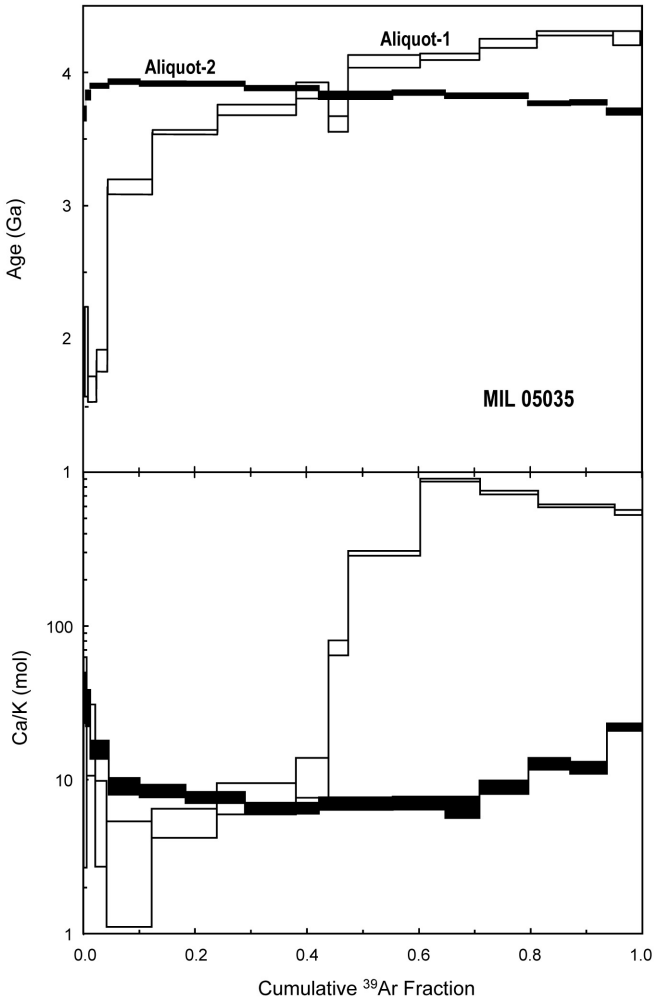

Fig. 6. Apparent age and Ca/K spectrum diagrams for two MIL 03035 bulk samples.

which previously gave an Ar-Ar age of 751 Ma (Torigoye-Kita et al. 1995). The maximum $^{40}Ar^*/^{39}Ar$ ages obtained by Torigoye-Kita et al. (1995; Table 1) during high temperature Ar release are between 3.9–4.3 Ga. The Ca/K ratios for Y-793169 plagioclase and bulk are similar and vary from 40 to 520 at high temperatures (Fig. 5). Comparison with the Ca/K values obtained from EMPA analyses (Table 2) suggests this was Ar released from a mixture of a high Ca/K phases (pyroxene) and a low Ca/K phase (possibly glass).

MIL 05035

The age and Ca/K spectrum diagrams of two bulk sample aliquots are shown in Fig. 6 and the results are summarized in Table 4. Aliquot-1 (9.23 mg) shows a disturbed age spectrum with a progressive increase in apparent age from ~1.6 Ga to 4.3 Ga. Aliquot-2 (3.85 mg) yielded a narrow range of apparent ages between 3.7–3.9 Ga. Summing the Ar released over all temperature steps for both samples gives similar integrated ages of 3.910 ± 0.012 Ga for aliquot-1 and 3.845 ± 0.014 Ga for aliquot-2. These are within error of the Rb-Sr and Sm-Nd ages of 3.90 ± 0.05 Ga and 3.80 ± 0.05 Ga, respectively (Nyquist et al. 2007). Since the K-Ar is more susceptible to disturbance than the Sm-Nd system, retention of a 4.3 Ga Ar-Ar age in the disturbed sample seems unlikely, and the pattern of ages may result from closed-system redistribution of ^{40}Ar released during a major impact shock event. It is interesting that previously the age spectrum obtained for Y-793169 by Torigoye-Kita et al. (1995) showed similarly high apparent ages of 4.3 Ga obtained from a plagioclase separate at high temperature which was, attributed to the presence of excess ^{40}Ar introduced during the shock event. MIL 05035 is a coarse-grained sample making it likely that the milligram-sized samples used in this study are not representative of the bulk mineralogy. This is probably the cause of the different Ca/K spectra (Fig. 6), with the disturbed sample having a high Ca/K phase dominating the Ar release at high temperature. This high Ca/K is absent from the undisturbed sample.

LAP 02205

The Ar-Ar age and Ca/K spectrum diagrams for LAP 02205 are shown in Fig. 7a, and the $^{40}Ar/^{36}Ar$ versus $^{39}Ar/^{36}Ar$ correlation in Fig. 7b. The age spectrum for bulk LAP 02205 (Fig. 7a) shows that the first ~51% of the $^{39}Ar_K$ release corresponds to an age of 3.047 ± 0.018 Ga. The following 49% of the $^{39}Ar_K$ release, corresponding to the intermediate and high temperature steps, shows a saddle shape, with an age of 2.908 ± 0.018 Ga. This is typical behavior associated with ^{39}Ar recoil. Summing Ar released over all temperature steps gives a total age of 2.985 ± 0.016 Ga. The Ca/K increases with temperature from ~10 to 250 (Fig. 7a). Comparison with EMPA data, suggest that the increase in Ca/K reflects a progressive release from plagioclase to pyroxene with increasing temperature.

Argon step heating of fragments with and without glassy vein material show similar age patterns. For the vein-bearing sample, the first 60% of $^{39}Ar_K$ release give consistent ages with an integrated value of 2.923 ± 0.076 Ga, slightly higher than the total age of 2.874 ± 0.056 Ga. The Ar release for the basalt fragment (without melt vein) has a total age of 2.889 ± 0.044 Ga. The consistent Ar-Ar ages obtained from different portions of LAP 022025 (Fig. 7b) indicates that the K-Ar system was not significantly disturbed during the shock event that led to the formation of melt veins.

NWA 479

The age and Ca/K spectrum diagrams for NWA 479 show good agreement with NWA 032 (Fig. 8), supporting the pairing relationships between these two meteorites. Following the interpretation of Ar data for NWA 032 (Fagan et al. 2002; Fernandes et al. 2003), the age spectrum of NWA 479 is considered to be influenced by ^{39}Ar-recoil. On this basis a total age of 2.721 ± 0.040 Ga is calculated for 90% $^{39}Ar_K$-release. This age is indistinguishable from the weighted

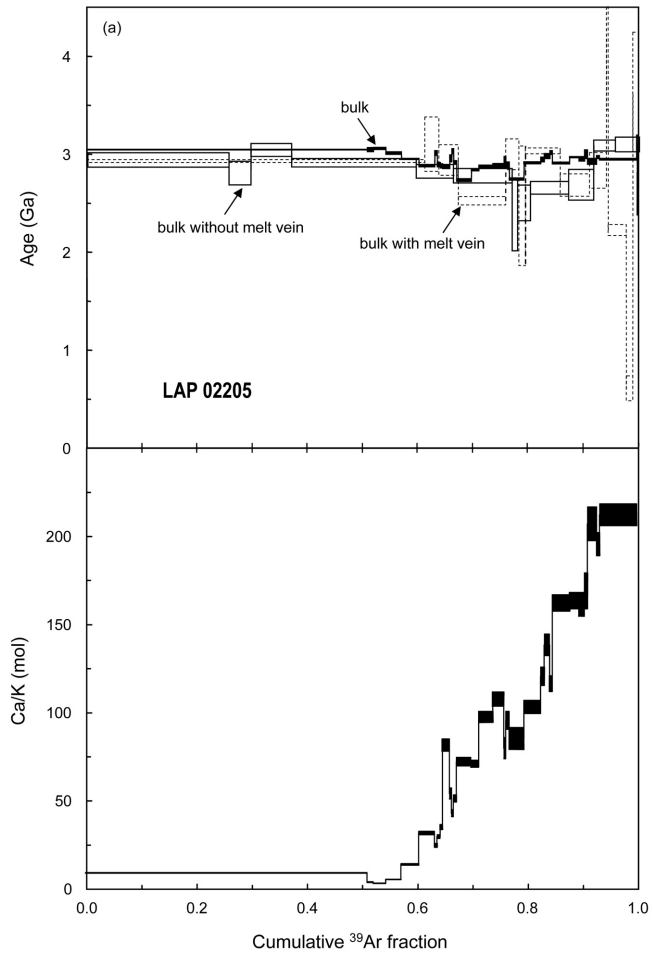

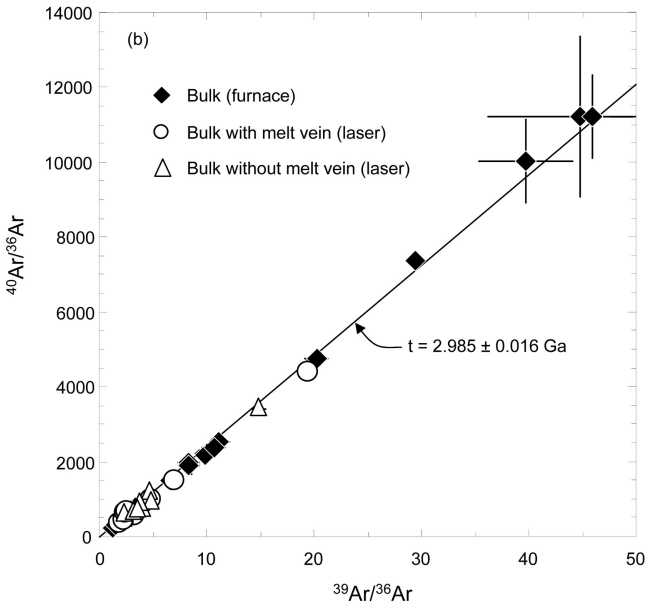

Fig. 7 Ar-Ar results for LAP 02205 for bulk, glass vein-bearing, and vein-free samples. a) Apparent age and Ca/K spectrum diagrams. b) ^{40}Ar/^{36}Ar versus ^{39}Ar/^{36}Ar diagram.

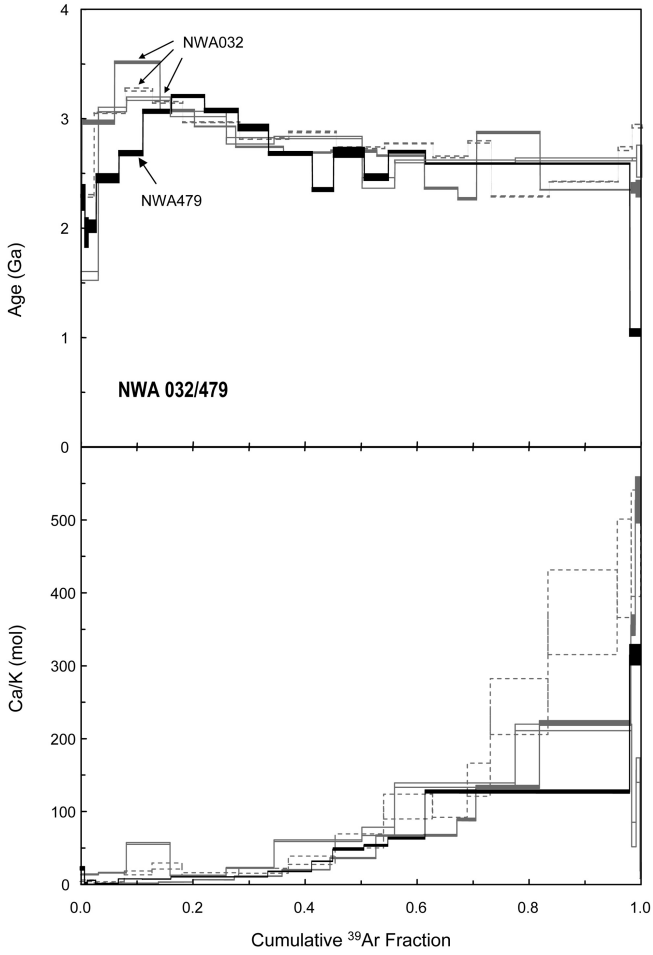

Fig. 8. Apparent age and Ca/K spectrum diagrams NWA 479 compared to results from three samples of NWA 032 published by Fernandes et al. (2003).

mean obtained from three samples of NWA 032 at 2.779 ± 0.056 Ga (Fernandes et al. 2003).

EET 96008

Figure 9 shows the age spectrum for bulk, basalt and breccia samples of EET 96008. All samples show variable effects of resetting with low apparent ages obtained over the initial 10–30% of ^{39}Ar release. The Ar loss may have occurred during an impact event 600–700 Ma, with the basalt sample being most affected (Fig. 9). All samples then show steep rises in apparent ages which level out at higher temperatures to give ages for the breccia of 3.755 ± 0.342 Ga (76% of $^{39}Ar_K$ release) and the basalt 2.650 ± 0.086 Ga (65% $^{39}Ar_K$ release). The bulk sample yields an intermediate age of 3.221 ± 0.020 Ga (72% of $^{39}Ar_K$ release) as anticipated assuming it contains both basalt and breccia components. The age obtained for the breccia sample is broadly comparable with the U-Pb isochron of 3.53 ± 0.27 Ga for apatite (Anand et al. 2003; Terada et al. 2005) and the ^{40}K-^{40}Ar gas retention ages determined by Eugster et al. (1996) of ~3.30 Ga. If the

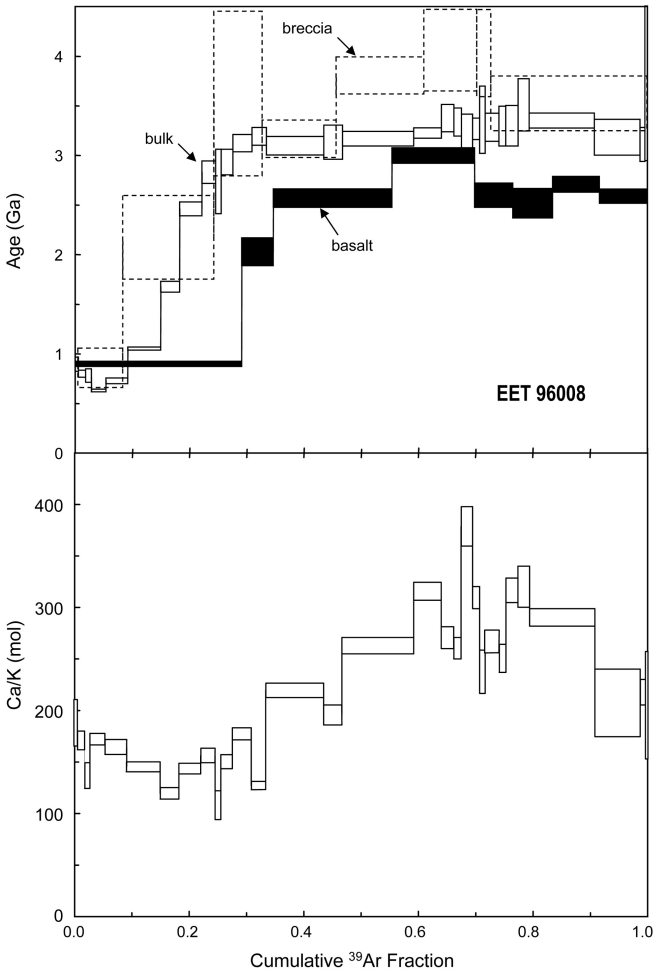

Fig. 9. Apparent age (bulk, basalt, and breccia portions) and Ca/K spectrum (bulk only) diagrams for EET 96008.

much younger age of the basalt in EET 96008 is interpreted as a crystallization age then the basalt and breccia components must have been assembled in their present form <2.65 Ga ago.

Summary of Ages and Comparison with Literature Data

The Ar-Ar ages reported for six meteorites studied are summarized in Table 4, literature data are given in Table 1 and all data are compared in Fig. 10. The Ar-Ar age of bulk and mineral separates from A-881757 are indistinguishable within error giving a weighted mean of 3.802 ± 0.080 Ga and overall the different isotopic ages of this meteorite are concordant at 3.8–3.9 Ga (Table 1, Fig. 10a). The age obtained for Y-793169 at 3.811 ± 0.098 Ga is similar to ages previously determined for this meteorite (Table 1, Fig. 10b). U-Pb and Pb-Pb systems give ages of 3.9 Ga, however the Sm-Nd age is discordant at 3.4 Ga (Torigoye-Kita et al. 1995). Mineralogical studies have shown that Y-793169 has been subjected to a shock event(s) and thermal annealing which is likely to have resulted in Ar loss (Mikouchi 1999a). Disturbance of K-Ar system of Y-793169 may be related to shock heating at ~200 Ma as suggested by the lowest apparent age obtained from the pyroxene/glass fraction. Shock would also account for the presence of recrystallized plagioclase which was converted to maskelynite followed by subsequent recrystallization of plagioclase during thermal annealing (Mikouchi 1999a).

Two bulk MIL05035 samples gave integrated age between 3.845 ± 0.014 and 3.910 ± 0.012 Ga. The ^{40}Ar-^{39}Ar for aliquot-1 suggests a disturbance in the K-Ar system and likely causing a closed-system redistribution of the ^{40}Ar. Thus, the 3.845 ± 0.014 Ga age is the preferred age. Nyquist et al. (2007) have determined similar Sm-Nd and Rb-Sr ages of 3.80 ± 0.05 Ga and 3.90 ± 0.04 Ga, respectively (Table 1) for MIL 03035. These ages are comparable to those determined for the related basalts A-881757 and Y-793169 (Misawa et al. 1993; Torigoye-Kita et al. 1995) and for the basaltic component of MET 01210 (Terada et al. 2007a), (Table 1). As shown in Fig. 10c, the Ar-Ar age of MIL03035 is concordant with previous isotopic age determination.

Previous age determinations for LAP 02205 are summarized in Table 1 and range between an Ar-Ar age of 2.95 ± 0.04 Ga and a Sm-Nd age of 3.15 ± 0.04 Ga (Nyquist et al. 2005; Rankenburg et al. 2007) and are indistinguishable from the Ar-Ar age of 2.985 ± 0.008 Ga obtained in this study. (Fig. 10d).

NWA 479 and NWA 032 have indistinguishable Ar-Ar ages of 2.779 ± 0.056 Ga 2.721 ± 0.040 Ga (Fernandes et al. 2003), respectively. The Ar-Ar age of NWA 032 is also concordant with the Rb-Sr and Sm-Nd ages (Table 1: Borg et al. 2007) making these meteorites among the youngest lunar basalts. Day et al. (2007) suggested that LAP 02205, NWA 032, and NWA 479 may be samples from a lava flow pile, where LAP 02205 was at a lower level and extruded first. The slightly older Ar-Ar age of LAP 02205 (2.985 ± 0.008 Ga; this study) compared to NWA 032/479 is consistent with this suggestion.

EET 96008 shows evidence for multiple age events some of which are reasonably concordant with previous ages determinations (Table 1 and Fig. 10e). This meteorite shows evidence of an impact event at ~630 Ma with a best estimate for the crystallization of the basaltic component of 2.650 ± 0.086 Ga. The Ar-Ar age for the breccia component is 3.755 ± 0.171 Ga and likely records the event that formed this portion of the meteorite. The latter age is in reasonable agreement with ion microprobe U-Pb age determinations in EET 96008 reported by Anand et al. (2003) who obtained 3.53 ± 0.27 Ga for apatite and 3.52 ± 0.10 Ga for merrilite. A similar age of 3.503 ± 0.140 Ga (U-Pb) was obtained for phosphates in the paired meteorite EET 87521 (Terada et al. 2005). The lithology from which the phosphates were extracted was not recorded in either of these previous studies, however the similarity of their U-Pb ages to Ar-Ar age of the

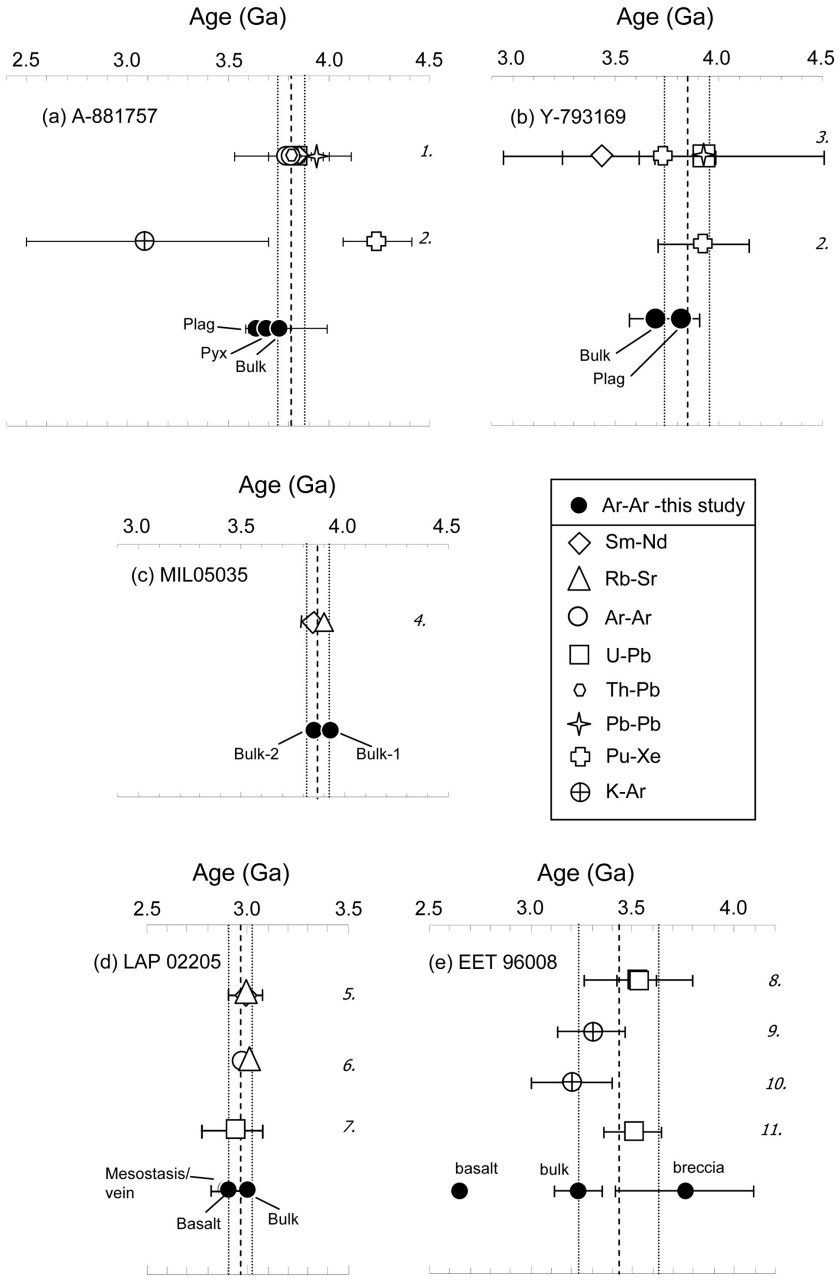

Fig. 10. Comparison of published age determinations with Ar-Ar ages reported in this study. a) A-881757. b) Y-793169. c) MIL 05035. d) LAP 02205. e) EET 96008. The dashed lined is the average age determined by combining all of the values, the dotted line is 1σ. Data sources: 1. Misawa et al. (1993); 2. Thalmann et al. (1996); 3. Torigoye-Kita et al. (1995); 4. Nyquist et al. (2007), 5. Rankenburg et al. (2007); 6. Nyquist et al. (2005); 7. Anand et al. (2005); 8. Anand et al. (2003); 9. Eugster et al. (1996); 10. Vogt et al (1993); 11. Terada et al. (2005);

breccia confirms their origin in the highland component as was suggested by Anand et al. (2003).

Cosmic Ray Exposure

Cosmic-ray exposure (CRE) ages have been determined using the $^{38}Ar/^{37}Ar_{Ca}$values for individual temperature steps, following minor correction for trapped ^{38}Ar based upon the ^{36}Ar release. Steps having $^{38}Ar/^{36}Ar$ higher than the cosmogenic ratio of 1.54 are assumed to contain neutron-derived ^{38}Ar from ^{37}Cl ($^{38}Ar_{Cl}$), these were usually from low temperature steps and have not been used for calculating CRE ages. The long period between irradiation and analysis means that $^{37}Ar_{Ca}$ had almost completely decayed in samples Y-793169 and A-881757 leading to imprecise CRE ages which are therefore not considered further. While most cosmogenic ^{38}Ar is produced from spallation of Ca in lunar basalts, there are significant contributions from other elements most

notably K, Ti, Cr, Mn, Fe, and Ni. To take account of this, the lunar surface (2π) production rates of $^{38}Ar_{Ca}$ have therefore been calculated from the bulk chemical composition of each basalt and the production rate equations of Eugster and Michel (1995). The bulk compositions are from published data: MIL 05035 (Joy et al. 2008), LAP 02205 (Joy et al. 2006), EET 96008 (Anand et al. 2003), and NWA 479 (Barrat et al. 2001). It is assumed that during the short transit time from the Moon to Earth (<1 Ma) there is negligible production of cosmogenic ^{38}Ar relative to that formed in the lunar regolith.

The production rate of $^{38}Ar_{Ca}$ in MIL 05035 is 1.021×10^{-8} cm^3 g^{-1} Ca Ma^{-1}. The CRE ages decline over the release probably due to heterogeneous release from different mineral phases in this coarse-grained basalt. The major Ca-release over the interval 1350–1650 °C is considered to be dominantly from plagioclase and gives CRE ages equivalent to 1–3 Ma exposure at the lunar surface. However, the data obtained from MIL 05035 aliquot-1 are also consistent with previous interpretations of the near-surface exposure age for A-881757 of <1 Ma and with Y-793169 exposed for 50 Ma at a shielding depth of 500 g/cm^2 (Thalman et al. 1996). Without measurements of any depth-dependant cosmic-ray isotopes it is not possible to choose between these different depth-exposure possibilities. However, it is notable that the cosmogenic ^{38}Ar concentration of MIL 03035 of $8.5 \pm 0.3 \times 10^{-9}$ cm^3/g is indistinguishable within error of $7.9 \pm 0.4 \times 10^{-9}$ cm^3/g obtained previously for Y-793169 (Thalman et al. 1996).

Most of the low temperature release steps from bulk LAP 02205 gave $^{38}Ar/^{36}Ar > 1.54$ and probably contain a contribution from $^{38}Ar_{Cl}$, as a result of terrestrial contamination. Eleven steps at higher temperature yielded CRE ages in the range 40–50 Ma obtained using a production rate of 1.086×10^{-8} cm^3 g^{-1} Ca Ma^{-1}, giving an integrated value of 43 ± 7 Ma.

The first six Ar release steps from the bulk sample of EET 96008 have $^{38}Ar/^{36}Ar > 1.54$ and are assumed to be influenced by the presence of $^{38}Ar_{Cl}$. Thereafter the value of this ratio decreases to between 1–1.5 considered to represent a mixture of trapped and cosmogenic Ar. Using a ^{38}Ar production rate for EET 96008 of 1.032×10^{-8} cm^3 g^{-1} Ca Ma^{-1}, the ^{38}Ar/Ca ratio of the remaining steps is equivalent to ~10 Ma of exposure at the lunar surface. Previously, Eugster et al. (2000) used cosmogenic ^{21}Ne and ^{126}Xe to show that EET 96008 had experienced a two stage exposure history, the first stage at a shielding depth of 200–600 g/cm^2 for 26 Ma and the second stage at 1–20 g/cm^2 depth for <9 Ma. Applying this two-stage exposure model to our results shows broad agreement except that the maximum exposure for the shallow burial stage is reduced to ≤4 Ma.

Argon released below 800 °C from NWA 479 yield $^{38}Ar/^{36}Ar > 1.54$ indicating the presence of $^{38}Ar_{Cl}$. At higher temperatures $^{38}Ar/^{36}Ar$ values range between the trapped and cosmogenic ratios. Using a production rate of 1.111×10^{-8} cm^3 g^{-1} Ca Ma^{-1}, the high temperature steps yield a CRE age of 275 ± 8 Ma. This is similar to the CRE age obtained for NWA 032 of 212 ± 11 Ma (Fernandes et al. 2003) again consistent with the proposed paired relationship of these two meteorites. On the basis of compositional, mineralogical, crystallization and CRE-age data for LAP 02205 and NWA 479, these meteorites appear to be part of a lava flow pile where LAP 02205 was at a lower level and extruded first followed by NWA 032 (CRE age = 212 Ma) and then NWA 479. CRE-age suggests a 2π surface exposure age for MIL 05035 of 1–3 Ma. The CRE-age obtained for high temperature heating steps of the gabbroic fragmental breccia EET 96008 is ~10 Ma.

Lunar Source Areas

The five meteorites analysed in this study, show a series of compositional and mineralogical affinities and distinctions from those of the Apollo and Luna mare basalts studied for the past four decades. Relative to the suggested regional sources of the six lunar basalt meteorites and considering their chemical composition, there seems to be a rather strong affinity of the lunar basaltic meteorites with the Apollo 12 and 15 olivine basalts, Apollo 15 pigeonite basalts and Apollo 14 high Al and K basalts (Fig. 1). There is on the other hand, in the present lunar basaltic meteorite collection, little similarity to basalts from Apollo 11 and Apollo 17 (Fig. 1). This may not be surprising as the area that shows a longer volcanic activity, based on surface ages obtained by crater counting (Hiesinger et al. 2000 and 2003) is within and adjacent to the incompatible-rich (and radioactive) Procellarum-KREEP terrain (PKT; Haskin 1998; Jolliff et al. 2000; Korotev et al. 2000), which makes it a long-lived heat source capable of sustaining melting in this area of the Moon (Hess and Parmentier 1999; Hess 2000; Head and Wilson 1992; Wieczorek et al. 2001; Fernandes and Burgess 2005). The most likely source area for these meteorites has been determined to be adjacent to within the PKT and a few close to the Apollo-Luna landing sites.

Knowledge of the source areas of lunar mare meteorites enables them to be placed into a planetary context in order to gain insight into lunar crustal and mantle evolution. This can help improve our current level of understanding into the degree of chemical and isotopic heterogeneity of the lunar mantle, the duration of volcanism, especially in the areas rich in heat producing elements which may have enabled a longer period of volcanism on the Moon, and any regional variations in the formation processes of the source regions and basalts. Here we suggest possible areas on the Moon for A-881757, Y-793169, MIL 05035, LAP 02205, EET 96008, and NWA 032/NWA 479 by combining the absolute ages of the meteorites with surface ages obtained by crater counts and global chemical maps obtained by orbiting spacecraft. The crater

count ages used are from Hiesinger et al. (2000 and 2003) and account is taken of the value and the 1σ error of the age determination for each meteorite. Mare flows are referred to by their letter and number codes used by Hiesinger et al. (2000, 2003). We also compare the chemical composition of the meteorites with the TiO_2, FeO, K, and Th maps produced from data obtained by the Clementine and Lunar Prospector missions. The TiO_2 map used is from Gillis et al. (2003) and maps of FeO, K and Th are from Gillis et al. (2004). It is important to note that the compositional maps obtained using orbital spacecraft are determining the composition of the regolith that has developed on top of the basalt flows over an area of 60 km per pixel (Gillis et al. 2004). The regolith may contain a significant proportion of non-local material and are typically different in composition from the basalts they are developed on by several percent (Gillis et al. 2004). With this limitation in mind, an exact match between meteorite composition and orbital chemical maps is unlikely with the present data and the concentrations of FeO, Th, K, TiO_2, of the meteorites are the best approximation for the composition of potential source on the lunar surface.

Age data obtained prior to the present work using different isotopic systems suggest that A-881757, Y-793169, and MIL 05035 most likely crystallized at ~3.9 Ga, making these among the oldest lunar basalts, comparable in age with basalts from Apollo 11 and 17 (Takeda et al. 1993; Warren and Kallemeyn 1993). Misawa et al. (1993) and Nyquist et al. (2007) have suggested that the only regions of the Moon having similar crater age and TiO_2 to A-881757, Y-793169 and MIL 05035 are in Mare Imbrium or Mare Humorum.

Due to the chemical and mineralogical compositional affinities demonstrated by the YAMM group (Joy et al. 2008, Arai et al. 2007; Ziegler et al. 2007) and similar ages A-881757 (3.87 ± 0.06 Ga; Misawa et al. 1993), Y-793169 (3.81 ± 0.22 Ga; Torigoye-Kita et al. 1995), and MIL 05035 (3.80 ± 0.05 Ga; Nyquist et al. 2007), a common source on the lunar surface is reported based on A-881757 age which shows the least disturbed Ar-Ar age spectra. The flows with corresponding ages are: Oceanus Procellarum (P15 and P36), Mare Nubium (N2), Mare Australe (A1, A13, A14 and A21), and Mare Humorum (H7). Compositionally, the most similar flow is H7 (concordant FeO, TiO_2 and Th) in the NW region of Mare Humorum. As mentioned above, A-881757 and Y-793169 have been suggested to be source paired, either Mare Imbrium (Misawa et al. 1993) or Mare Humorum (Nyquist et al. 2007).

Nyquist et al. (2005) suggested the following broad list of source areas for LAP 02205, Mare Insularum, Mare Cognitum, or Mare Nubium, further west in south central Oceanus Procellarum, or in west central Mare Imbrium. The Apollo 12 and 15 landing sites have been mentioned by Anand et al. (2006), Day et al. (2005), Joy et al. (2006), Mikouchi et al. (2004), Righter et al. (2005) and Zeigler et al. (2005). Ages determined for LAP 02205 are 2.985 ± 0.016 Ga (this study; and Nyquist et al. 2005) and 3.15 ± 0.07 Ga (Nyquist et al. 2005), thus lavas corresponding to either age were identified. Lavas corresponding to the younger age are present in Oceanus Procellarum (P26, P28 and P29), Mare Insularum (IN4) and Mare Imbrium (I23). Older age, lava flows are present in Oceanus Procellarum (P20, P21, P22 and P23), Mare Insularum (IN4), Mare Nubium (N15 and N16), Mare Australe (A21 and A30), Mare Humorum (H11), Mare Serenitatis (S24), and Mare Imbrium (I18 and I19). Comparing compositional data, it appears that TiO_2 concentrations do not match in several of the above flows, the most comparable surface composition for the younger age of LAP 02205 is P29 (all four elements are concordant), and for the older age of LAP 02205 it is P21 and I19. Considering the suggestion that these two ages correspond to two different volcanic episodes of the same source (Nyquist et al. 2005) and the proximity of flow P29 and P21, we suggest the likely source for LAP 02205 to be the NW region of Oceanus Procellarum.

Only Mare Imbrium has lava flows (I27 and I28; Hiesinger et al. 2000) similar to the Ar-Ar age determined for the basalt component of EET 96008 of 2.650 ± 0.43 Ga. The small lava flow I27 is located on the northern area of Mare Imbrium and show concordant FeO and TiO_2, but no compositional match for Th and K. Flow I28 is larger and located on the NW region of Mare Imbrium, and the only match found was with TiO_2. The previous suggestion for a source region for this meteorite was given by Arai et al. (2005) to be within the Procellarum KREEP Terrain.

For basalt NWA 032 and NWA 479, only one flow with comparable age (2.779 ± 0.056 Ga; best estimate based on data by Fernandes et al. [2003]) was found adjacent to Mare Imbrium (I25), inside Plato crater. However, comparing the chemical composition of NWA 032/NWA 479 with elemental maps, shows that abundances for FeO and TiO_2 in Plato Crater are not comparable.

CONCLUSIONS

The unbrecciated lunar basalt meteorite Y-793169 (3.811 ± 0.098 Ga) represents one of the oldest lunar basalt rocks in the world collection and comparable to samples from Apollo 11. The pattern of argon release suggests a disturbance at 203 ± 42 Ma also evidenced by the existence of glass reported by Mikouchi (1999). A-881757 is classified as gabbroic mare basalt and shows a coarse grain texture unlike most mare basalts. This sample shows the existence of maskelynite which suggests that it was subjected to pressure <45 GPa. However, there is no evidence for disturbance of the K-Ar system, and a ^{40}Ar-^{39}Ar crystallization age of 3.763 ± 0.046 Ga is determined. MIL 05035 is a coarse-grained VLT mare gabbro comprising pyroxene, plagioclase and mesostasis the age spectrum shows evidence for partial disturbance giving an integrated age of 3.845 ± 0.015 Ga

similar Sm-Nd and Rb-Sr ages obtained by Nyquist et al. (2007; Table 1) These ages are comparable to those determined for the related basalts A-881757 and Y-793169. Ar-Ar ages presented here for Y-793169, A-881757, and MIL 05035 are within error of those determined by different isotopic systematics, Sm-Nd, U-Pb Th-Pb, Pb-Pb and Rb-Sr (Figs. 10a–c; Tables 1 and 4).

A crystallization age of 2.985 ± 0.008 Ga was determined for bulk rock of the unbrecciated lunar mare basalt LAP 02205. This age is in agreement with ages determined using other isotopic systematics (Fig. 10d; Nyquist et al. 2005; Anand et al. 2006; Rankenburg et al. 2007). The three fragments analysed from basaltic fragmental breccia EET 96008 show evidence for a disturbance at ~631 Ma at the low temperature steps. The age obtained for the breccia and basalt components are 3.755 ± 0.171 Ga and 2.650 ± 0.086 Ga, respectively.

The crystallization age of 2.734 ± 0.040 Ga determined for the unbrecciated basalt NWA 479 is indistinguishable from NWA 032 of 2.779 ± 0.056 Ga (Ar-Ar age; Fernandes et al. 2003); and 2.852 ± 0.065 Ga (Rb-Sr age; Borg et al. 2007) supporting the paired relationship of these two meteorites.

To place the five meteorites (A-881757, Y-793169, MIL 05035, LAP 02205, EET 96008, and NWA 479) in a planetary context, a systematic comparison was carried out using the isotope ages and chemical compositions of the meteorites and the cratering ages of lava flows (Hiesinger et al. 2000, 2003) and element maps (FeO, TiO_2, K, and Th) obtained by the Lunar Prospector mission (Gillis et al. 2003 and 2004) of the lunar surface. Using Hiesinger et al. (2000, 2003) nomenclature, the likely source for A-881757, Y-793169, and MIL 05035 is flow H7 within Mare Humorum, for LAP 02205 the westernmost flows within Oceanus Procellarum P29 and P31, and for NWA 032/479 (2.779 ± 0.056 Ga) flow I25 in Mare Imbrium. A possible source for EET 96008 includes flows I27 or I 28 found in the Mare Imbrium; however the present data set is not conclusive.

Acknowledgments–We thank Dr. Hideyasu Kojima at NIPR for providing the samples of Asuka 881757 and Yamato 793169, and Dr. Martin Bizzarro at the Geological Institute and the Geological Museum of Copenhagen, Denmark, provided samples LAP 02205 and EET 96008 for this study. Sample MIL 05035 was kindly provided by the Meteorite Working Group. Tomoko Arai from the National Institute of Polar Research is thanked for kindly providing mineral major element data of Asuka 881757 and Yamato 793168. We are grateful for the helpful comments from Don Bogard and Mario Trieloff, and for comments by Ryan Zeigler on an earlier version of this manuscript. The writing of this paper has benefited from NASA ADS Proceedings Query Service at http://adsabs.harvard.edu/proceedings_service.html, and from the Lunar Meteorite List website created and maintained by Dr. Randy Korotev at Washington University in St. Louis, Missouri, USA, http://meteorites.wustl.edu/lunar/moon_meteorites_list_alumina.htm. This work was funded by the Fundação para a Ciência e a Tecnologia, Portugal and the STFC, UK.

Editorial Handling—Dr. Timothy Swindle

REFERENCES

Anand M., Taylor L. A., Neal C. R., Snyder G. A., Patchen A., Sano Y., and Terada K. 2003. Petrogenesis of lunar meteorite EET 96008. *Geochimica et Cosmochimica Acta* 67:3499–3518.

Anand M., Taylor L. A., Floss C., Neal C., Terada K., and Tanikawa S. 2006. Petrology and geochemistry of La Paz Icefield 02205: A new unique low-Ti mare-basalt meteorite. *Geochimica et Cosmochimica Acta* 70:246–264.

Arai T., Takeda H., and Warren P. H. 1996. Four lunar meteorites: Crystallization trends of pyroxenes and spinels. *Meteoritics & Planetary Science* 31:877–892.

Arai T., Shimoda H., Kita N., Morishita Y., and Kojima H. 2005. Source magma compositions for basalt clasts of lunar meteorite EET 87521 in connection to KREEP (abstract #5196). 68th Annual Meeting of the Meteoritical Society. *Meteoritics & Planetary Science* 40. CD-ROM.

Arai T., Misawa K., and Kojima H. 2007. Lunar meteorite MIL 05035: Mare basalt paired with Asuka-881757 (abstract #1582). 30th Lunar and Planetary Science Conference. CD-ROM.

Barrat J. A., Chaussidon M., Bohn M., Gillet Ph., Göpel C., and Lesourd M. 2005. Lithium behavior during cooling of a dry basalt: An ion-microprobe study of the lunar meteorite Northwest Africa 479 (NWA 479). *Geochimica et Cosmochimica Acta* 69: 5597–5609.

Borg L. E., Shearer C. K., Asmerom Y., and Papike J. J. 2004. Prolonged KREEP magmatism on the Moon indicated by the youngest dated lunar igneous rock. *Nature* 432:209–211.

Borg L., Gaffney A., and DePaolo D. 2007. Rb-Sr & Sm-Nd isotopic systematics of NWA 032 (abstract #5232). 70th Annual Meeting of the Meteoritical Society. *Meteoritics & Planetary Science* 42. CD-ROM.

Burgess R. and Turner G. 1998. Laser ^{40}Ar-^{39}Ar age determinations of Luna 24 mare basalts. *Meteoritics & Planetary Science* 33: 921–935.

Day J. M. D., Pearson D. G., and Taylor L. A. 2005. ^{187}Re-^{187}Os isotope disturbance in La Paz mare basalt meteorites (abstract #1424). 36th Lunar and Planetary Science Conference. CD-ROM.

Day J. M. and Taylor T. A. 2007. On the structure of mare basalt lava flows from textural analysis of the LaPaz Icefield and Northwest Africa 032 lunar meteorites. *Meteoritics & Planetary Science* 42: 3–17.

Eugster O. and Michel Th. 1995. Common asteroid breakup events of eucrites, diogenites, and howardites, and cosmic-ray production rates for noble gases in chondrites. *Geochimica et Cosmochimica Acta* 59:177–199.

Eugster O., Thalmann Ch., Albrecht A., Herzog G. F., Delaney J. S., Klein J., and Middleton R. 1996. Exposure history of glass and breccia phases of lunar meteorite EET 87521. *Meteoritics & Planetary Science* 31:299–304.

Eugster O., Polnau E., Salerno E., and Terribilini D. 2000. Lunar surface exposure models for meteorites Elephant Moraine 96008 and Dar al Gani 262 from the Moon. *Meteoritics & Planetary Science* 35:1177–1181.

Fagan T. J., Taylor G. J., Keil K., Bunch T. E., Wittke J. H.,

Korotev R. L., Jolliff B. L., Gillis J. J., Haskin L. A., Clayton R. N., Mayeda T. K., Fernandes V. A., Burgess R., Turner G., Eugster O., and Lorenzetti S. 2002. Northwest Africa 032: Product of lunar volcanism. *Meteoritics & Planetary Science* 37:371–394.

Fernandes V. A., Burgess R., and Turner G. 2000. Laser ^{40}Ar-^{39}Ar studies of Dar al Gani 262 lunar meteorite. *Meteoritics & Planetary Science* 35:1355–1364.

Fernandes V. A., Burgess R., and Turner G. 2003. ^{40}Ar-^{39}Ar chronology of lunar meteorites Northwest Africa 032 and 773. *Meteoritics & Planetary Science* 38:555–564.

Fernandes V. A. and Burgess R. 2005. Volcanism in Mare Fecunditatis and Mare Crisium: Ar-Ar studies. *Geochimica et Cosmochimica Acta* 69:4919–4934.

Gillis J. J., Jolliff B. L., and Elphic R. C. 2003. A revised algorithm for calculating TiO_2 from Clementine UVVIS data: A synthesis of rock, soil, and remotely sensed TiO_2. *Journal of Geophysical Research*, 108 (E2), 3–1, 5009, doi:10.1029/2001JE001515.

Gillis J. J., Jolliff B. L., and Korotev R. L. 2004. Lunar surface geochemistry: Global concentrations of Th, K, and FeO as derived from lunar prospector and Clementine data. *Geochimica et Cosmochimica Acta* 68:3791–3805.

Hagerty J. J., Shearer C. K., and Vaniman D. T. 2006. Heat-producing elements in the lunar mantle: Insights from ion microprobe analyses of lunar pyroclastic glasses. *Geochimica et Cosmochimica Acta* 70:3457–3476.

Haloda J., Tycova P., Korotev R. L., Fernandes V. A., Burgess R., Jakes P., Gabzdyl P., and Kosler J. 2009. Petrology, geochemistry, and age of low-Ti mare-basalt meteorite Northeast Africa 003-A: A possible member of the Apollo 15 mare basaltic suite. *Geochimica et Cosmochimica Acta* 73:3450–3470.

Haskin L. A. 1998. The Imbrium impact event and the thorium distribution at the lunar highlands surface. *Journal of Geophysical Research* 103**:**1679–1689.

Haskin L. A. 1998. The Imbrium impact event and the thorium distribution at the lunar highlands surface. *Journal of Geophysical Research* 103:1679–1689.

Head J. W. and Wilson L. 1992. Lunar mare volcanism: Stratigraphy, eruption conditions, and the evolution of secondary crusts. *Geochimica et Cosmochimica Acta* 56:2155–2175.

Hess P. C. and Parmentier E. M. 1999. Asymmetry and timing of mare volcanism (abstract #1300). 30th Lunar and Planetary Science Conference. CD-ROM.

Hess P. C. 2000. On the source regions for mare picrite glasses. *Journal of Geophysical Research* 105**:**4347–4360.

Hiesinger H., Jaumann R., Neukum G., and Head J. W. 2000. Ages of mare basalts on the lunar nearside. *Journal of Geophysical Research* 105(E12): 29,239–29,275.

Hiesinger H. and Head, J. W. 2003. Ages and stratigraphy of mare basalts in Oceanus Procellarum, Mare Nubium, Mare Cognitum, and Mare Insularum. *Journal of Geophysical Research,* 108: 5065, doi:10.1029/2002JE001985.

Jolliff B. L., Gillis J. J., Haskin L. A., Korotev R. L., and Wieczorek M. A. 2000. Major lunar crustal terranes: Surface expressions and crust-mantle origins. *Journal of Geophysical Research* 105(E2):4197–4216.

Jolliff B. L., Korotev R. L., Ziegler R. A., and Floss C. 2003. Northwest Africa 773: Lunar mare breccia with a shallow-formed olivine-cumulate component, inferred very-low-Ti (VLT) heritage, and a KREEP connection. *Geochimica et Cosmochimica Acta* 67:4857–4879.

Jourdan F., Verati C., and Féraud G. 2006. Intercalibration of the Hb3gr ^{40}Ar/^{39}Ar dating standard. *Chemical Geology* 231:177–189.

Joy K. H., Crawford I. A., Downes H., Russel S. S., and Kearsley A. T. 2006. A petrological, mineralogical, and chemical analysis of the lunar mare basalt meteorite LaPaz Icefield 02205, 02224, and 02226. *Meteoritics & Planetary Science* 41:1003–1025.

Joy K. H., Crawford I. A., Anand M., Greenwood R. C., Franchi I. A., and Russell S. S. 2008. The petrology and geochemistry of Miller Range 05035: A new lunar gabbroic meteorite. *Geochimica et Cosmochimica Acta* 72:387–402.

Koeberl C., Kurat G., and Brandstätter F. 1993. Gabbroic lunar mare meteorites Asuka-881757 (Asuka-31) and Yamato 793169: Geochemical and mineralogical study. *Proceedings of the NIPR Symposium on Antarctic Meteorites* 6:14–34.

Korotev R. L. 1998. Concentration of radioactive elements in lunar materials. *Journal of Geophysical Research* 103**:**1691–1701.

McBride K., Satterwhite C., McCoy T., and Welzenbach L. 2003. Antarctic Meteorite Newsletter 26.

Mikouchi T. 1999a. Shocked plagioclase in the lunar meteorites Yamato-793169 and Asuka-881757: Implications for their shock and thermal histories. *Proceedings of the NIPR Symposium on Antarctic Meteorites* 12:151–167.

Mikouchi T. 1999b. Mineralogy and petrology of a new lunar meteorite EET 96008: Lunar basaltic breccia similar to Y-793274, QUE 94281 and EET 87521 (abstract #1558). 30th Lunar and Planetary Science Conference. CD-ROM.

Mikouchi T., Chokai J., Arai T., Koizumi E., Monkawa A., and Miyamoto M. 2004. LAP 02205 lunar meteorite: Lunar mare basalt with similarities to the Apollo 12 ilmenite basalt (abstract #1300). 35th Lunar and Planetary Science Conference. CD-ROM.

Misawa K., Tatsumoto M., Dalrymple G. B., and Yanai K. 1993. An extremely low U/Pb source in the Moon: U-Th-Pb, Sm-Nd, Rb-Sr, and ^{40}Ar/^{39}Ar isotopic systematics and age of lunar meteorite Asuka 881757. *Geochimica et Cosmochimica Acta* 57:4687–4702.

Nishiizumi K., Arnold J. R., Caffee M. W., Finkel R. C., Southon J. M. and Reedy R. C. 1992. Cosmic ray exposure histories of lunar meteorites Asuka 881757, Yamato 793169, and Calcalong Creek. *Proceedings of the NIPR Symposium on Antarctic Meteorites* 7:129–132.

Nishiizumi K., Masarik J., Caffee M. W., and Jull A. J. T. 1999. Exposure histories of paired lunar meteorites EET 96008 and EET 87521 (abstract #1980). 30th Lunar and Planetary Science Conference. CD-ROM.

Nyquist L. E., Shih C.-Y., Reese Y., and Bogard D. D. 2005. Age of lunar meteorite LAP 02205 and implications for impact-sampling of planetary surfaces (abstract #1374). 36th Lunar and Planetary Science Conference. CD-ROM.

Nyquist L. E., Shih C.-Y., and Reese Y. 2007. Sm-Nd and Rb-Sr andes for MIL 05035: Implications for surface and mantle sources (abstract #1702). 38th Lunar and Planetary Science Conference. CD-ROM.

Rankenburg K., Brandon A. D., and Norman M. D. 2007. A Rb–Sr and Sm–Nd isotope geochronology and trace element study of lunar meteorite LaPaz Icefield 02205. *Geochimica et Cosmochimica Acta* 71:2120–2135.

Righter K., Collins S. J., and Brandon A. D. 2005. Mineralogy and petrology of the La Paz Icefield lunar mare basaltic meteorites. *Meteoritics & Planetary Science* 40:1703–1722.

Shih C.-Y., Nyquist L. E., Reese Y., and Bischoff A. 2008. Sm-Nd and Rb-Sr isotopic studies of meteorite Kalahari 009: An old VLT mare basalt (abstract #2165). 39th Lunar and Planetary Science Conference. CD-ROM.

Schwarz W. H. and Trieloff M 2007. Intercalibration of ^{40}Ar–^{39}Ar age standards NL-25,HB3gr hornblende, GA1550, SB-3, HD-B1 biotite and BMus/2 muscovite. *Chemical Geology* 24:2218–231.

Sokol A. K., Fernandes V. A., Schulz T., Bischoff A., Burgess R., Clayton R. N., Münker C., Nishiizumi K., Palme H., Schultz L., Weckwerth G., and Mezger K. 2008. Geochemistry, petrology and ages of the lunar meteorites Kalahari 008 and 009: New

constraints on early lunar evolution. *Geochimica et Cosmochimica Acta* 72:4845–4873.

Stöffler D. and Grieve R. 2007. Impactites. In *Metamorphic rocks: A classification and glossary of terms*, edited by D. Fettes and J. Demonds. Cambridge University Press. pp. 82–91.

Takeda H., Arai T. And Saiki K. 1993. Mineralogical studies of lunar meteorites Y-793169, a mare basalt. *Proceedings of the NIPR Symposium on Antarctic Meteorites* 6:3–13.

Terada K., Saiki T., Oka Y., Hayasaka Y., and Sano Y. 2005. Ion microprobe U-Pb dating of phosphates in lunar basaltic breccia, Elephant Moraine 87521. *Geophysical Research Letters* 32: L20202, doi:10.1029/2005GL023909.

Terada K., Anand M., Sokol A. K., Bischoff A., and Sano Y. 2007a. Cryptomare magmatism 4.35 Gyr ago recorded in lunar meteorite Kalahari 009. *Nature* 450:849–852.

Terada K., Sasaki Y., Anand M., Joy K. H., and Sano Y. 2007b. Uranium–lead systematics of phosphates in lunar basaltic regolith breccia, Meteorite Hills 01210. *Earth and Planetary Science Letters* 259:77–84.

Thalmann C., Eugster O., Herzog G. F., Klein J., Krähenbühl U., Vogt S., and Xue S. 1996. History of lunar meteorites Queen Alexandra Range 93069, Asuka 881757, and Yamato 793169 based on noble gas isotopic abundances, radionuclide, and chemical composition. *Meteoritics & Planetary Science* 31:857–868.

Torigoye N., Misawa K., and Tatsumoto M. 1993. A low U/Pb source in the Moon: U-Th-Pb systematics of lunar meteorite Yamato 793169. *Proceedings of the NIPR Symposium on Antarctic Meteorites* 6:58–75.

Torigoye-Kita N., Misawa K., Dalrymple G. B., and Tatsumoto M. 1995. Further evidence for a low U/Pb source in the Moon: U-Th-Pb, Sm-Nd, and Ar-Ar isotopic systematics of lunar meteorite Yamato-793169. *Geochimica et Cosmochimica Acta* 59:2621–2632.

Turner G. 1971. ^{40}Ar-^{39}Ar dating: The optimization of irradiation parameters. *Earth and Planetary Science Letters* 10:227–234.

Vogt S., Herzog G. F., Eugster 0., Michel TH., Niedermann S., Krähenbühl U., Middleton R., Dezfouly-Arjomandy B., Fink D., and Klein J. 1993. Exposure history of the lunar meteorite, Elephant Moraine 87521. *Geochimica et Cosmochimica Acta* 57: 3793–3799.

Warren P. H. and Kallemeyn G. W. 1989. Elephant Moraine 87521: The first lunar meteorite composed of predominantly mare material. *Geochimica et Cosmochimica Acta* 53:3323–3300.

Warren P. and Kallemeyn 1993. Geochemical investigation of two lunar mare meteorites: Yamato-793169 and Asuka-881757. *Proceedings of the NIPR Symposium on Antarctic Meteorites* 6: 35–57.

Warren P. H. and Ulff-Møller F. 1999. Lunar meteorite EET 96008: Paired with EET 87521, but rich in diverse clasts (abstract #1450). 31st Lunar and Planetary Science Conference. CD-ROM.

Wieczorek M. A., Zuber M. T., and Phillips R. J. 2001. The role of magma buoyancy on the eruption of lunar basalts. *Earth and Planetary Science Letters* 185:71–83.

Yanai K. 1991. Gabbroic meteorite Asuka-31; Preliminary examination of a new type of lunar meteorite in the Japanese collection of Antarctic meteorites. Proceedings, 21st Lunar and Planetary Science Conference. pp. 317–324.

Yanai K. and Kojima H. 1991. Variety of lunar meteorites recovered from Antarctica. *Proceedings of the NIPR Symposium on Antarctic Meteorites* 4:70–90.

Yanai K., Kojima H., and Naraoka H. 1993. The Asuka-87 and Asuka-88 collections of Antarctic meteorites; Search, discoveries, initial processing, and preliminary identification and classification. *Proceedings of the NIPR Symposium on Antarctic Meteorites* 6:137–147.

Zeigler R. A., Korotev R. L., Jolliff B. L., and Haskin L. A. 2005. Petrography and geochemistry of the LaPaz Icefield basaltic lunar meteorite and source crater pairing with Northwest Africa 032. *Meteoritics & Planetary Science* 40:1073–1101.

Zeigler R. A., Korotev R. L., and Jolliff B. L. 2007. Miller Range 05035 and Meteorite Hills 01210: Two basaltic lunar meteorites, both likely source-crater paired with Asuka 881757 and Yamato 793169 (abstract #2110). 38th Lunar and Planetary Science Conference. CD-ROM.